AstroSat: II. Highlights of Scientific Results From 2015–2021*

Science From AstroSat

Kulinder Pal Singh

AstroSat, launched in 2015, has observed all kinds of objects in the universe in X-rays and UV light. These objects range from isolated stars to stars in clusters, binary stars with compact companions like neutron stars and black holes, star-forming regions in the galaxies, and supermassive black holes in active nuclei of galaxies. In addition, it has carried out deep surveys of certain parts of the sky, reaching the farthest and the faintest objects in those regions. In this second part of the article, I highlight some of the important results obtained using AstroSat in the first five years of its operation.

Kulinder Pal Singh is an X-ray Astronomer who has worked on balloon, rocket and satellite borne X-ray telescopes and detectors for astronomy. He carries out multi-wavelength observations and data analysis. He developed India's first X-ray focusing telescope for *AstroSat* at TIFR, Mumbai. He is an INSA Senior Scientist at IISER, Mohali after retiring from TIFR in 2017.

1. Introduction

AstroSat[1], India's first astronomy satellite launched on 28 September 2015, has carried out a multitude of observations in the UV and X-rays using its five scientific instruments. It has observed stars in open and globular clusters, X-ray binaries containing compact objects like black holes, neutron stars and white dwarfs, galaxies and active galactic nuclei (AGN). Here, I describe some of the discoveries and important results obtained by AstroSat since its launch. The choice of results presented here is subjective, and the division into sections below is arbitrary. I will first describe the discoveries made principally with Ultra Violet Imaging Telescope (UVIT), followed by the discoveries made using the unique capability of studying simultaneous broad-band X-ray emission, followed by multi-wavelength studies using AstroSat. It should

[1] See K P Singh, AstroSat. I, *Resonance*, Vol.27, No.4, pp.513–528, April 2022.

*Vol.27, No.6, DOI: https://doi.org/10.1007/s12045-022-1391-5

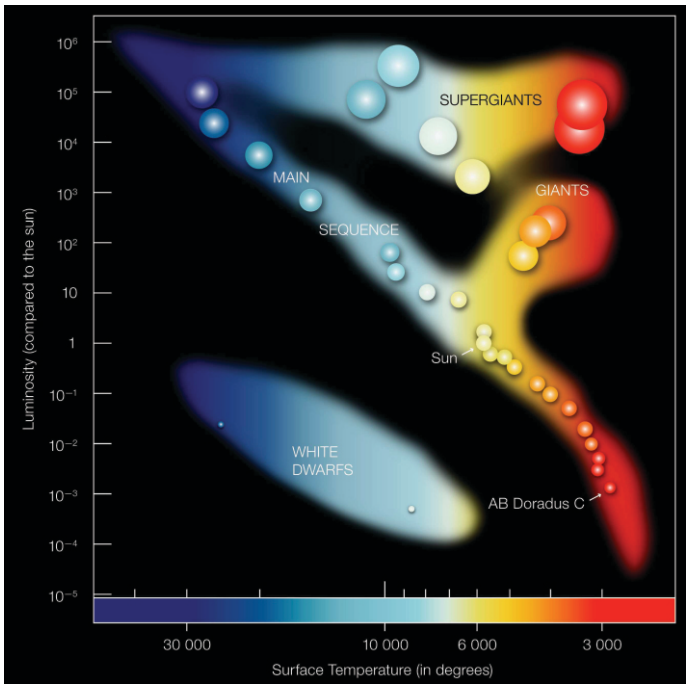

Figure 1. An example of an HR Diagram. (Copyright ESO)

be noted that the far UV (FUV) camera operating in the UVIT on AstroSat covers the wavelength range that is currently not accessible by any other telescope in the world.

To understand and put in general perspective the discoveries made with the Ultra-Violet Imaging Telescope, we need to know a little about stars and their life cycles, which are the important constituents of galaxies.

Keywords
AstroSat, X-rays, ultraviolet, stars, X-ray binaries, galaxies, active galactic nuclei.

The evolution and life cycles of stars are studied using the Hertzsprung–Russell (HR Diagrams), which are snapshots of the brightness of stars measured as absolute magnitudes plotted against their colors, which indicate their surface temperatures.

2. Stars and Their Life Cycles

The evolution and life cycles of stars are studied using the Hertzsprung–Russell (HR Diagrams), which are snapshots of the brightness of stars measured as absolute magnitudes plotted against their colors, which indicate their surface temperatures (T) (see *Figure* 1). The colors are quantified as a spectral sequence, with the hottest being called O-stars and the coolest being the M-stars (B, A, F, G, and K being of intermediate temperatures from hot to cold).

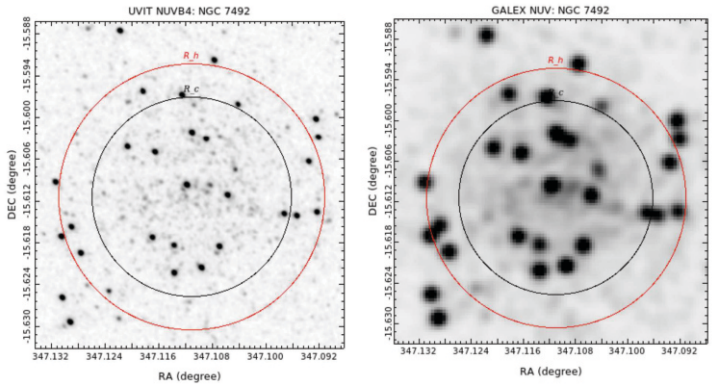

Figure 2. UVIT NUVB4 (effective wavelength = 263.2 nm, left) and GALEX NUV (eff. wavelength = 230.4 nm, right) images of NGC 7492. The red circle denotes the half light radius of 1.15 arcmin and the black circle denotes the core radius of 0.86 arcmin) of the cluster. (Credits: R Kumar et al., 2021 [1].)

The location of stars on this diagram basically depends on their masses. Their surface temperatures also depend on their sizes (shown as circles in *Figure* 1), which in turn depend on the phase of evolution they are in when observed. Most of the stars spend most of their life in the 'main sequence' (MS)—in the neighborhood where our Sun appears. Hot stars (shown in bluer shades in *Figure* 1) with T≥10000 K emit more UV radiation than the cooler stars, simply based on the expectation from black-body radiation as a function of temperature. These include massive supergiants, giants, and highly evolved white dwarfs near the end of their life cycle, as shown in *Figure* 1. However, even cool stars can produce a lot of UV and very soft X-rays from their upper atmospheres high above their surfaces—their chromospheric and coronal regions.

Therefore, by studying UV and soft X-ray emissions of stars, we are mainly tracking these types of stars. Stars are also known to aggregate in clusters, mainly of two types—globular and open. Globular clusters (GCs) contain mostly old stars. In a given cluster, the stars would have co-evolved (i.e., of similar ages) from the same parent material and are at the same distance from us, thereby providing insights into star formation from the interstellar medium. Stars in GCs also have very little interstellar extinction, thus providing a clearer view.

Stars are also known to aggregate in clusters, mainly of two types—globular and open.

UV Emission From Globular and Open Clusters

The UV light comes from hot and luminous stars, and the UVIT aboard AstroSat is particularly suited to finding such a population of stars in clusters. Its spatial resolution of 1.3 arcsec is especially useful for studying fields crowded with such stars as in GCs.

The UV light comes from hot and luminous stars, and the UVIT aboard AstroSat is particularly suited to finding such a population of stars in clusters. Its spatial resolution of 1.3 arcsec is especially useful for studying fields crowded with such stars as in GCs. In this respect, UVIT is well ahead of its predecessor instrument like GALEX (Galaxy Evolution Explorer, 2003–2013)[2] A comparison of the quality of data obtained from AstroSat and GALEX is shown in *Figure* 2 for a cluster known as NGC 7492.

Some of the really hot and luminous stars are post-asymptotic giant branch stars (pAGB), blue straggler stars (BSs), extreme blue and blue horizontal branch stars (EHBs, BHBs), white dwarfs (WDs), etc., straddling the intermediate regions of the HR diagram shown in *Figure* 1. Many GCs, viz., NGC 1261, NGC 2808, NGC 4147, NGC 7492, etc., have been observed with the UVIT, and many new BHB, EHB, and BS stars have been identified in them. *Figure* 3 shows a multi-color image of NGC 2808 made from stars detected in the NUV and FUV filters. The existence of these types of hot stars is very intriguing and extremely important for the study of UV emission from elliptical galaxies. These hot stars occur in a region above the turn-off point of the MS in the HR diagrams of star clusters, where no stars are expected based on the standard stellar evolution of co-evolving stars. It has been speculated that such stars result from stellar collisions or mass exchange in close binary systems.

[2] http://www.galex.caltech.edu/index.html.

It is well known that about two-thirds of the stars in a galaxy are in binary or multiple star systems. Since the multiple star systems can have different masses, they follow their own different evolutionary trajectories, except when they are too close, leading to a mass exchange between them and thus influencing and affecting each other's evolution leading to various outcomes.

Binary systems with evolved companions have been detected in several GCs and some old open clusters of stars. Open clusters have the advantage of relatively low stellar density, which helps identify binary systems that can be studied in detail and,

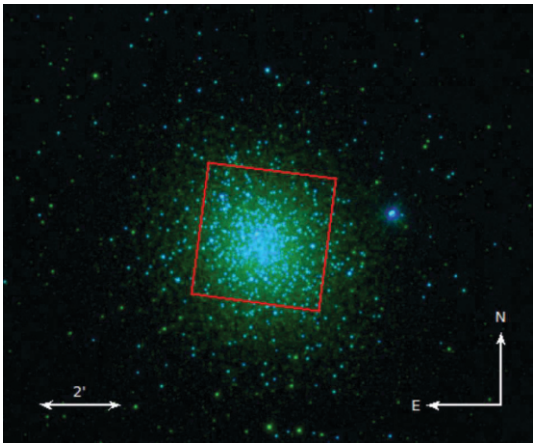

Figure 3. UVIT image of NGC 2808 with stars detected in the F154W filter (154 nm central wavelength in FUV) shown in blue, and those detected in the N242W filter (242 nm central wavelength in NUV) shown in green. The Hubble Space Telescope wide-field camera, which covers the inner 2.7×2.7 arcmin^2 region of the cluster, is marked in red. (Credits: D S Prabhu et al., 2021 [2].)

thus, help us understand the properties of binary systems in a tidally non-disruptive environment. AstroSat has observed several open clusters with the UVIT. These include Berkeley 67, King 2, NGC 2420, NGC 2477, NGC 2682 (M67), and NGC 6940. UVIT observations have been able to find and detect several BS stars and even identify low-mass white dwarf companions for some of them in an old (4.2±0.2 Gyr) open cluster, M67 [3].

AstroSat has also observed several late-type, rapidly-rotating, and coronally-active nearby stars with UVIT and SXT and detected simultaneous flaring activity in UV and X-rays [4–6]. These stars are potential candidates for hosting habitable planets around them, where the existence of life forms depends critically on the UV and X-ray emissions of the stars.

AstroSat has also observed several late-type, rapidly-rotating, and coronally-active nearby stars with UVIT and SXT and detected simultaneous flaring activity in UV and X-rays.

Star Formation in Galaxies

Galaxies in our local universe come in mostly three varieties—spirals, ellipticals (E), and lenticulars (known as SOs) in the famous Hubble tuning fork diagram. Spirals are mostly blue and young and usually host an abundance of cold gas, while E/SOs are mostly red and host little cold gas and dust. Ongoing star formation gives the galaxies their blue color. The UV emission is one of the best tracers of current star formation in galaxies for the reasons given above.

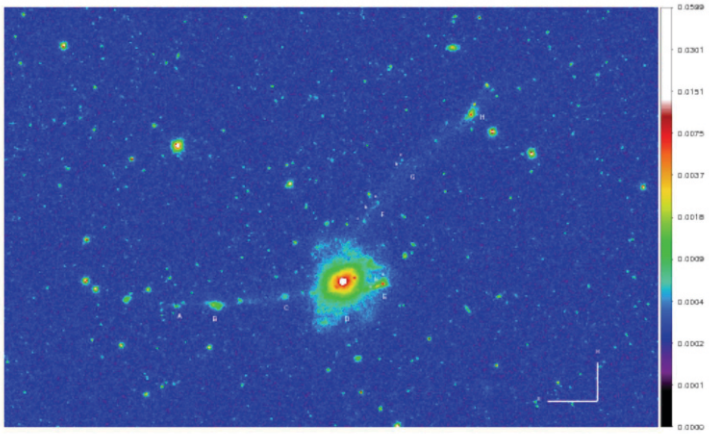

Figure 4. UVIT-NUV image of post-merger galaxy NGC 7252 showing the low surface brightness tidal tails. The tails extend up to 100 kpc, several times the size of the galaxy. (Credits: K George et al., 2018 [7].)

Mergers of galaxies can also lead to enhanced star formation, and it can be traced through tidal tails created by mergers.

An AstroSat-NUV image of a galaxy that shows signs of a merger of two spirals having taken place is shown in *Figure* 4. Large tails from the merged spirals can be seen here, and the enhanced blue color in the central region of the merged galaxy shows signs of renewed star formation in *Figure* 5.

Galaxies in Dense Environments.

Clusters of galaxies are the largest structures seen in the universe, where 100s to 1000s of galaxies are held together in a large and deep gravitational potential well defined by their total mass, which is dominated by dark matter. Their cores are very densely populated with galaxies, and most of the red galaxies (E/SOs) are located therein. In contrast, most of the blue galaxies (spirals) are found in low-density regions or outside the clusters of galaxies. The dense environment seems to suppress star formation activity leading to redder colors and change of morphology due perhaps to processes, such as strangulation, harassment, and ram pressure stripping, acting alone or in combination. These processes can convert star-forming spiral galaxies on the outskirts of a cluster into non-star-forming E/SOs when they are pulled into the core of

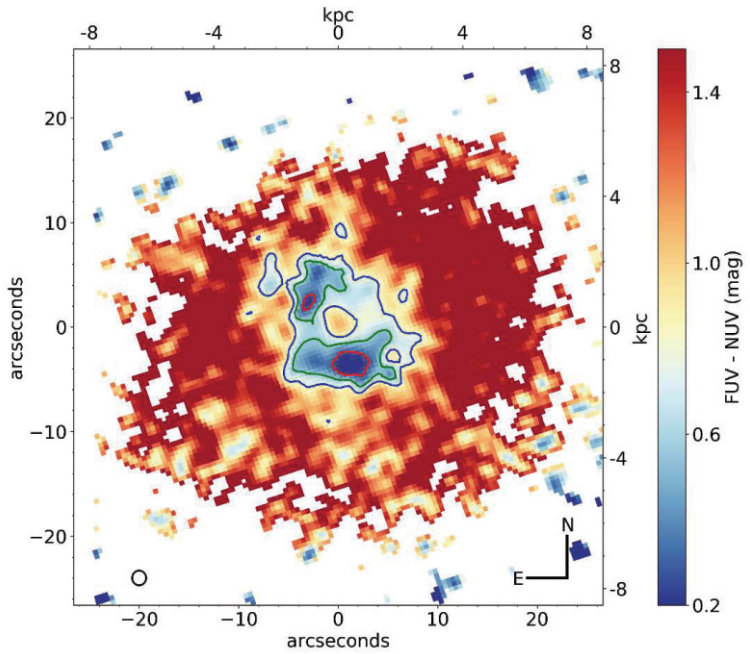

Figure 5. UVIT FUV-NUV color map of the central parts of NGC 7252 corresponding to the physical size of ~16 kpc on each side. Overlaid contours represent star-forming regions of the age of 150 (red), 250 (green), and 300 (blue) Myr to isolate regions of constant age. The blue ring in the center hosts young (150 Myr) stars compared to the rest of the galaxy. (Credits: K George et al., 2018 [8].)

a potential well. This can also result in some special morphologies, e.g., the shape of a jellyfish. One such example imaged with AstroSat-UVIT is shown in *Figure* 6.

Star Formation in the Early Epochs of the Universe from Deep Field Surveys

One of the most important findings with AstroSat has come from a very long observation of a chosen field in the UV. Known as deep field surveys, these cover parts of the sky bereft of any bright stars that could blind us to that part of the sky. Such surveys were first initiated by the Hubble Space Telescope (HST) in the early 1990s and then followed by all the space observatories operating at different wavelengths. These surveys are repositories of data from observations of all kinds of objects in the sky, reaching the faintest objects and the farthest ends of the universe, and are known to throw up surprises and discover new types of galaxies.

One of the most important findings with AstroSat has come from a very long observation of a chosen field in the UV. Known as deep field surveys, these cover parts of the sky bereft of any bright stars that could blind us to that part of the sky.

The AstroSat UV Deep Field (AUDF) explored a big chunk of

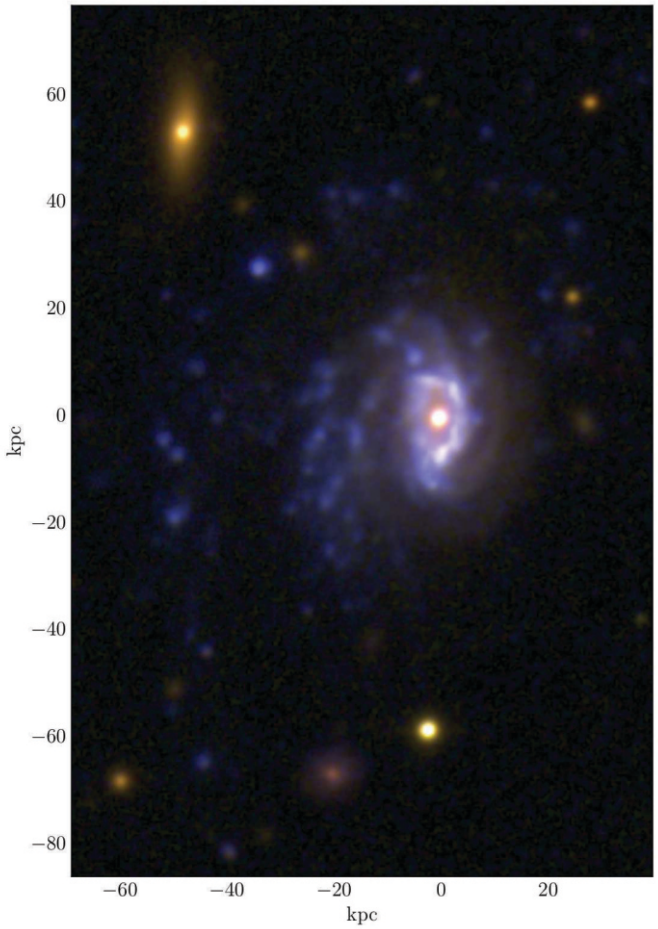

Figure 6. UVIT-NUV (blue) and optical (WINGS—WIde-field Nearby Galaxy-cluster Survey—B (red), V (green)) composite image of the jellyfish galaxy in Abell 85 cluster of galaxies. Diffuse emission and the knots of star formation in the stripped material from the galaxy can be seen clearly. The bright source at the center is an active galactic nuclei (AGN). The image is of size $\sim 100 \times 150$ arcsec^2. (Credits: K George et al., 2018 [9].)

The wavelength range of the FUV camera on AstroSat captures the light coming from ionized hydrogen, viz., Lyman continuum.

the sky which encompassed the one covered previously with the Chandra X-ray Observatory in X-rays and the HST in the optical region. The wavelength range of the FUV camera on AstroSat captures the light coming from ionized hydrogen, viz., Lyman continuum, that can leak out from some irregular clumpy galaxies at a distance given by redshifts (z) in the range of 0.4–2.5. This range of redshift is very important for the study of the formation of galaxies in the early universe during a very important phase of the early universe known as the re-ionization era.

Re-ionization era is when the first sources of light (stars) formed and released ionizing radiation in the intergalactic medium, re-

heating the gas and changing its opacity. To observe, measure, and quantify how many of these ionizing photons escape from the galaxies and thus understand what kind of stars formed in the early universe is one of the most challenging problems today.

The radiation coming from galaxies that are farther away ($z > 2.5$) can be seen using other wavelength bands—optical, infrared, etc., with other space or ground-based observatories. However, for observing galaxies at lower redshifts, one needs to observe at shorter wavelengths from space observatories.

AUDF is the deepest (most sensitive) UV field imaged so far, spanning a range of distances (redshifts). Putting this field together with high astrometric accuracy using data from AstroSat that is continuously drifting while in orbit around the Earth has required painstaking efforts over a couple of years by astronomers working on these data.

AUDF is the deepest (most sensitive) UV field imaged so far, spanning a range of distances. Putting this field together with high astrometric accuracy using data from AstroSat that is continuously drifting while in orbit around the Earth has required painstaking efforts over a couple of years by astronomers working on these data.

After carefully going through several hundred objects in the field, it has led to the discovery of a clumpy galaxy named ADUFs01 at $z = 1.42$ close to the peak ($z \sim 1.6$) of the cosmic star formation history. The redshift measurements of the galaxy came from the Hubble Space Telescope, involving collaborators from abroad. This is the first such galaxy to be found emitting Lyman continuum between $0.4 < z < 2.5$ (previously known as the deserted region for Lyman continuum leakers) and highlights the uniqueness of AstroSat/UVIT.

The large fraction of escaping Lyman continuum photons observed is a very important parameter in cosmological simulations and will profoundly impact processes leading to the formation of galaxies. The work continues further to expand the depth of coverage and find more such examples. The details of the study have been published in *Nature Astronomy* by Saha et al., [10].

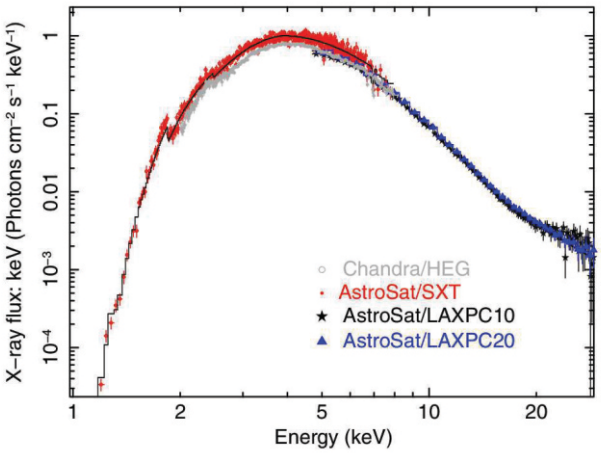

Figure 7. Broadband X-ray spectrum of 4U 1630-47—a black hole X-ray binary from AstroSat SXT, LAXPC, and Chandra High Energy Grating. All X-ray spectra have been fitted with a common model. (Credits: S Bhattacharyya et al., 2021 [11], and M. Pahari [12].)

3. Studies of Broad-band X-ray Emission

X-ray Spectra of Compact Binaries

The brightest X-ray sources in our galaxy are the X-ray binaries with a compact companion accreting matter from an ordinary star and supernova remnants.

The brightest X-ray sources in our galaxy are the X-ray binaries with a compact companion accreting (gravitationally pulling) matter from an ordinary star and supernova remnants. The compact companion is either a neutron star (NS) or a black hole (BH) in the case of the brightest objects and a white dwarf in the case of their cousins with much less brightness—generally referred to as cataclysmic variables. The star from which matter is accreted can be a main sequence star, giant star, or red dwarf. X-ray binaries with an NS or a BH are further classified based on the mass of the companion star as Low-Mass X-ray Binaries (LMXBs) or High-Mass X-ray Binaries (HMXBs). The matter being accrued has fairly high angular momentum. Therefore, to conserve angular momentum, it first forms an accretion disk and then falls onto the surface of a compact companion. In the case of the compact companion being an NS, the material is channeled by very strong (billions to trillions of Gauss) magnetic field lines before falling to the NS's surface, while in the case of a BH, it goes through an event horizon. The accretion disk can extend quite close to the event horizon in the case of a BH. The matter that is accrued gets very hot (millions to billions of degrees Kelvin), gets ion-

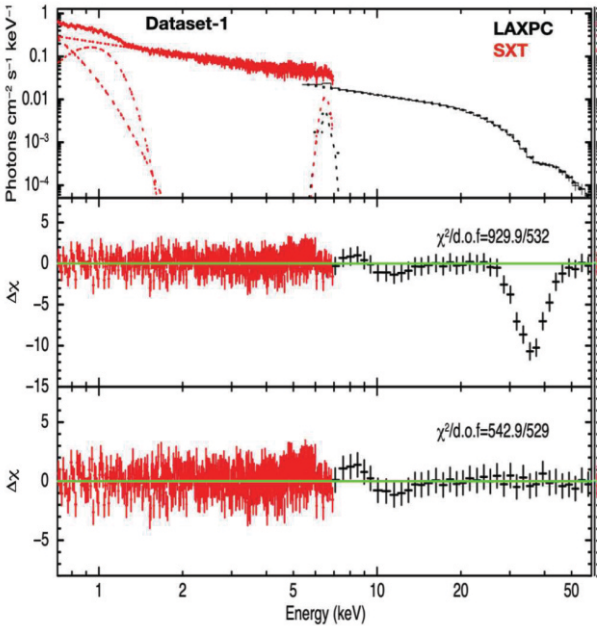

Figure 8. The broadband X-ray spectrum of Her X-1 observed by AstroSat SXT (red) and LAXPC (black). The unfolded spectrum (top panel) shows different model components. The cyclotron absorption line is shown in the middle panel after fitting with the best continuum model plus CRSF and then setting the depth of CRSF to zero and looking at the residuals. The lowest panel shows the best fit with CRSF included. (Credits: Bala et al., 2020 [13].)

ized, and produces X-rays. X-rays are emitted from the accretion disk and hot spots on/near the NS surface and from close to the event horizon in the case of a BH.

The capability to measure X-ray spectra spanning a very broad energy range of 0.3–30 (sometimes extending to 80 keV) simultaneously with the SXT, LAXPC, and CZTI has been used quite extensively to model the emission processes in several X-ray binaries. For example, 4U 1630–47, a binary with a black hole, was observed with AstroSat during its 2016 outburst and found to be in a very soft state with an accretion disk contribution of ~97% to the total flux. The spectral modeling (see *Figure* 7) was used to estimate the inner edge radius of the disk and to measure the black hole spin parameter. An absorbed, relativistic, disk blackbody model with Gaussian absorption features and a Comptonization model were used for fitting the data (including data from Chandra High Energy Grating) shown in *Figure* 7 to derive the dimensionless black hole spin parameter to be 0.92±0.04 with 99.7% confidence [12]. Similarly, observations of the broadband

The capability to measure X-ray spectra spanning a very broad energy range of 0.3–30 (sometimes extending to 80 keV) simultaneously with the SXT, LAXPC, and CZTI has been used quite extensively to model the emission processes in several X-ray binaries.

X-ray spectrum of LMC X-1—a black hole binary in the Large Magellanic Cloud, led to the measurement of the black hole spin parameter of ~0.93 [14].

In X-ray binaries containing neutron stars with strong magnetic fields, the accreting matter follows the magnetic field lines of the neutron star to its magnetic poles.

In X-ray binaries containing neutron stars with strong magnetic fields, the accreting matter follows the magnetic field lines of the neutron star to its magnetic poles. The accretion column thus formed produces an X-ray emission affected by the magnetic field. This interaction gives rise to absorption features in the X-ray spectra known as 'cyclotron resonant scattering features' (CRSFs) or 'cyclotron lines'. These require careful measurement of the X-ray continuum afforded by the combined broadband response of all the co-aligned AstroSat X-ray detectors. The study of cyclotron lines enables the determination of the neutron star's magnetic field. AstroSat has measured cyclotron line energies from Her X-1 (the first X-ray source from which such a line was discovered in 1976), 3A 1822-371, 4U 1907+09, GRO J2058+42, 4U 1538-52, and a binary pulsar in the Small Magellanic Cloud during its outburst in late 2017. One such measurement of the CRSF is shown in *Figure* 8 (from [13]).

Rhythmic and Arrhythmic Heartbeats of Compact X-ray Binaries

X-rays emitted from compact X-ray binaries carry signatures of rhythmic spin periods and orbital periods, irregular (arrhythmic) fluctuations and instabilities in the accretion disk flows, and sporadic burning of accumulated matter on the surfaces through thermonuclear reactions. Some of these signatures are quasi-periodic (QPO) with frequencies close to kilo-Hertz (KHz). The hard X-ray detectors (LAXPCs) with a time resolution of 10μs study these time signatures to understand the accretion processes in these binaries. High-frequency QPOs are observed in the ~1 Hz to ~1 kHz range in LMXBs, while low-frequency QPOs of ~10 to 100 mHz have been detected mostly in HMXBs, particularly in transient sources.

One such transient X-ray source observed immediately after the

launch of AstroSat is 4U 0115+63. This observation led to the discovery of QPOs at 1 mHz and 2 mHz frequencies, probably associated with instabilities in the accretion disk around the neutron star.

One of the important sources studied with AstroSat is GRS 1915+105, containing a black hole. Observations carried out during its transition from a non-variable state to a periodic flaring state dubbed as heartbeat oscillations of 3–5 Hz led to the discovery of another intermediate state when the large-amplitude, irregular variability of the order of thousands of seconds turned into a 100–150 s nearly periodic flares before transiting to the heartbeat state. The light curves in the 4–50 keV energy band and the power density distribution as a function of frequency are shown in *Figure* 9.

Another finding made possible due to the simultaneous broadband spectral coverage of AstroSat combined with temporal information is the discovery of a correlation between the QPO frequency and the inner radius of the accretion disk and accretion rate. The frequency divided by the accretion rate varies as a function of the inner accretion disk radius as predicted decades ago by the relativistic standard accretion disk theory for a rapidly spinning black hole with a spin parameter of ~0.9. Details of this and more such examples are given in [15].

AstroSat has studied a large number of X-ray binaries of all types listed above. It has measured the evolution of spin periods of accreting pulsars from a variety of binary systems like 3A 1822-371, 4U 1909+07, 4U 1907+09, 4U 0728-25, SAX J1748.9-2021, GRO J2058+42, 3A 0726-260, Swift J0243.6+6124, etc. It has carried out measurements of pulse shapes or patterns of heartbeats at different energies, extending them to the highest X-ray energies (80–200 keV) for the first time. An ultraluminous X-ray pulsar, known as Swift J0243.6+6124 is one of them [16].

Thermonuclear Bursts and Novae

In a binary system containing a neutron star or a white dwarf, as the accreted material piles up on the hot degenerate surface

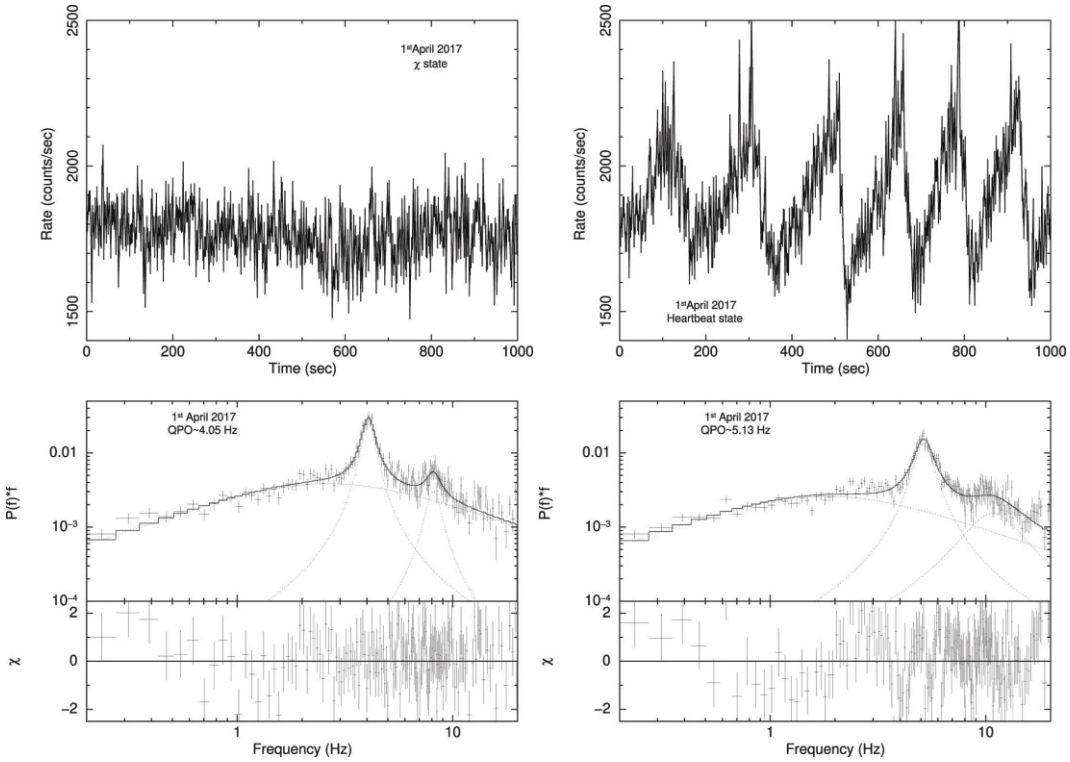

Figure 9. Light curves of GRS 1915+105 in hard X-rays in 2.0 sec bins for 1000 s observations in two variability states known as the χ class and heartbeat state (top panel). The corresponding power density spectrum in 0.2–20.0 Hz range are shown in bottom panels. (Credits: Misra et al., 2020 [17].)

and increases in mass, the temperature increases until explosive thermonuclear burning of the hydrogen and helium-rich material ensues. In neutron star binaries, such an explosive burning manifests as bursts known as Type-I bursts. A similar eruption in a white dwarf binary leads to a thermonuclear runaway (TNR) condition and an eruption that is seen as a nova. Type-I bursts are characterized by a sharp increase in X-ray intensity within 0.5–5.0 sec and exponential decay in ~10–100 sec.

Using AstroSat-LAXPC, Roy et al., [19] have presented a time-resolved (0.5 s time-bin) spectroscopy of 12 Type-I X-ray bursts in 4U 1636-536. The temperatures and radii obtained as a function of time indicate a photospheric radius expansion (PRE) during 2 of these bursts. They detect burst oscillations at 581 YHz in three bursts.

On the other hand, Novae can continue to glow for several days

and months after the initial outburst.

The TNR ejects and pushes the material from the surface at high velocities (> 300 kms^{-1}). The photosphere of the WD expands, and the optically-thick ejecta around it results in a rapid increase in luminosity, resulting in emission and absorption features from within complex ejecta of unknown structure. In the meantime, steady nuclear burning continues on the WD surface in quasi-hydrostatic equilibrium until the accrued fuel source is finished. At this stage, the ejecta becomes optically thin, and the photosphere recedes back to the WD, starting to reveal strong emission peaking in soft X-rays. When the ejecta becomes transparent before the nuclear burning ends, an underlying 'super-soft X-ray source' (SSS) is usually seen. An example emergence of such SSS that was caught with the SXT for a recurrent nova, known as V3890 Sgr, that erupted on 2019 August 27.87. This eruption happened after 28 years and was observed with the AstroSat as shown in *Figure* 10. The reasons for a strong X-ray variability observed with AstroSat SXT (*Figure* 10) at this stage at timescales of minutes to hours is still a mystery (see [18] for more details).

X-ray Polarization Measurements

One of the most difficult and least attempted measurements in X-ray astronomy is the polarization of X-rays. The only reliable measurement obtained so far is for the pulsar (a rotating neutron star) in the Crab Nebula—remnant of a massive stellar explosion known as a supernova, observed in 1054 AD. CZTI aboard AstroSat has performed X-ray polarization measurements of the Crab pulsar at different rotation phases of the pulsar—a first. This study suggests that the polarization shows maximum variation during the 'off-pulse' duration when no contribution from the pulsar is expected, posing a serious challenge to most of the current theories of X-ray production in the pulsar. These results have been published in *Nature Astronomy* by Vadawale et al., [20].

CZTI aboard AstroSat has performed X-ray polarization measurements of the Crab pulsar at different rotation phases of the pulsar—a first.

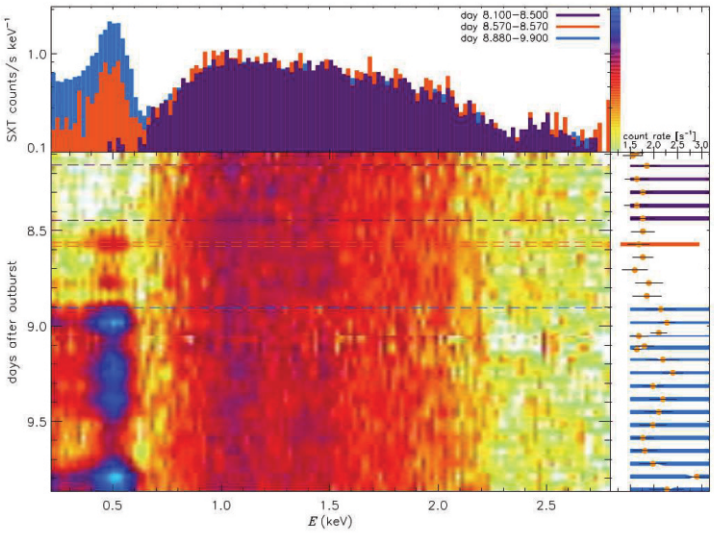

Figure 10. V3890 Sgr—a recurrent nova observed with the SXT showing its spectral evolution in the middle panel with elapsed observing time along the vertical axis and photon energy on the horizontal axis, on the same scales as the light curve on the right and the spectra on top, respectively. (Credits: Singh et al., 2021 [18].)

4. Multi-wavelength Studies of Active Galactic Nuclei

Active Galactic Nuclei are the engines that power the nuclear or central region of galaxies. These are the most powerful sources of electromagnetic (em) radiation in the universe, covering all the wavelengths.

Active Galactic Nuclei (AGN) are the engines that power the nuclear or central region of galaxies. These are the most powerful sources of electromagnetic (em) radiation in the universe, covering all the wavelengths, from radio to γ-rays, and dominate the sky beyond our Milky Way galaxy. There are several types depending on their observational properties. Most are weak in radio and are called radio-quiet (RQ) AGN or QSOs (quasi-stellar objects), and their less powerful cousins are known as Seyfert galaxies, and these are also closer to us. Only ~10% are strong radio sources that also contain powerful large scale (kpc to Mpc) jets. The objects that have their jets presumably pointed directly at us (observers) are known as blazars or BL Lac objects, named after their highly variable prototype—BL Lac. There are also subtypes known as flat-spectrum radio quasars (FSRQs), high polarization quasars (HPQs), high peak energy BL Lacs (HBLs), low peak energy BL Lacs (LBLs), etc., (see [21] and [22] for more details of different AGN types).

A supermassive black hole (SMBH) is believed to exist at the cen-

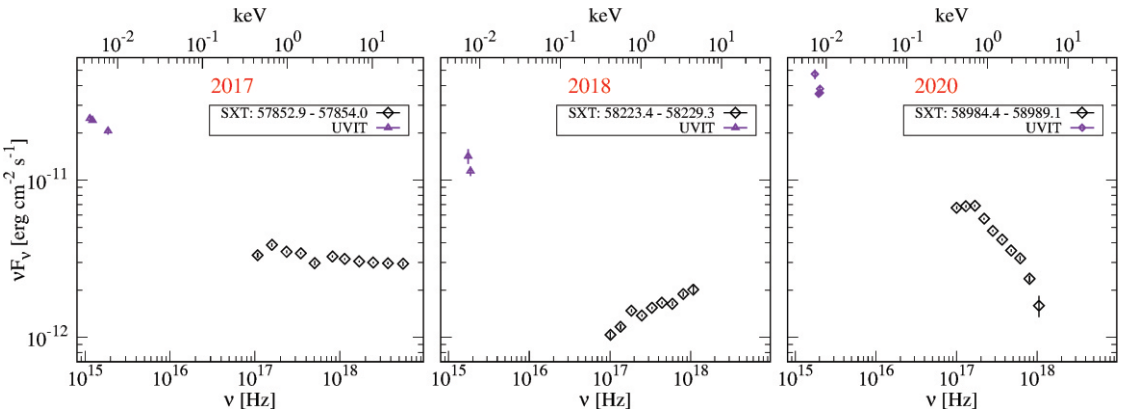

Figure 11. Simultaneous UV and soft X-ray observations of a blazar OJ 287 with AstroSat. (Credits: Kushwaha et al., 2021 [23].)

ter of these AGN and is the source of all radiation (isotropic and from a jet) powered by the accretion of matter from the surroundings.

The UV and soft X-ray radiation are emitted mostly from the inner parts of the accretion disc, but some of it may be associated with radio jets.

In RQ AGN, the emission in X-rays is dominated by a power law component believed to originate from a hot corona surrounding the SMBH. In addition, an energy cutoff in hard X-rays above 60–80 keV, fluorescent line emission from iron between 6 and 7 keV, a hard energy bump above 10 keV due to Compton reflection of the power-law, and very soft X-ray component below 1 keV from an accretion disk are also observed. The outer parts of the accretion disk contribute to optical-FUV emission. AstroSat has carried out multiple observations of many Seyfert galaxies and over a dozen blazars of different types.

In a Seyfert galaxy known as IC 4329A, observed five times with it AstroSat in 2017, it appears that the variability amplitude is larger in the UV band than in the X-ray bands [24]. This suggests that UV emission from the accretion disk is the primary driver and not the illumination of the disk by X-rays. The seed photons from UV emission act as the primary seed photons for the hot corona, producing broadband soft and hard X-ray continuum via thermal

In a Seyfert galaxy known as IC 4329A, observed five times with it AstroSat in 2017, it appears that the variability amplitude is larger in the UV band than in the X-ray bands.

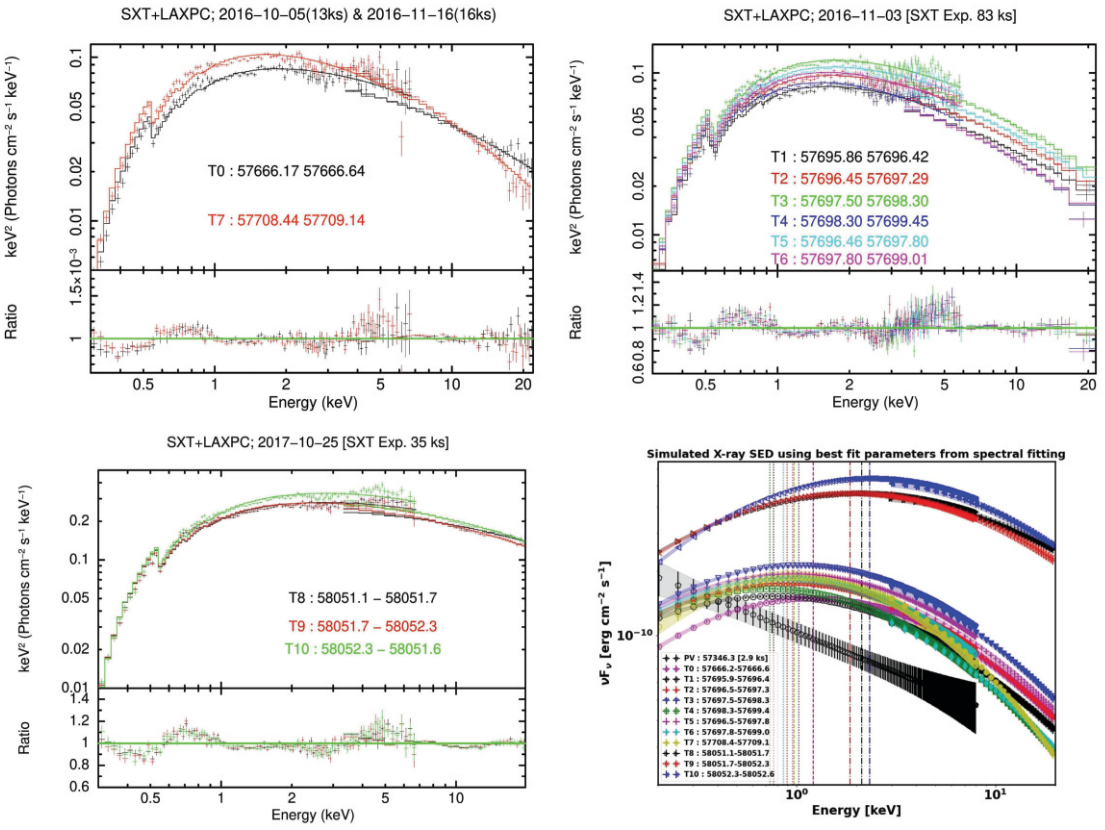

Figure 12. Simultaneous soft and hard X-ray observations of 1ES 1959+650 with AstroSat. (Credits: Chandra et al., 2021 [25].)

Comptonization that is observed. The X-ray spectral variability can be explained as due to the cooling of hot corona from kT_e ~42 keV to ~32 keV as the UV flux increases, while the optical depth remains constant at $\tau \sim 2.3$ (see [24] for more details).

The most famous blazar observed is OJ 287, believed to contain a binary system of SMBH. This object was observed with AstroSat from 2017 to 2020 and was caught in three very different flux states tracing its source spectral evolution.

Spectral energy distribution (SED) of blazars, have two very broad-band humps—one which is believed to be produced via synchrotron emission in the infrared to soft X-rays, and the other via inverse Compton (IC) scattering emission, dominating the hard X-ray to γ-rays. The IC component is believed to come from the scattering of soft photons originating from the local synchrotron radiation within the jet, producing the synchrotron self-Compton (SSC) component, or it could originate from the nuclear IR/optical/UV emission producing the external Compton (EC) component. All

AGN are highly variable across the entire electromagnetic spectrum and require simultaneous multiwavelength observations to understand their nature and underlying physical processes. AstroSat allows us to observe AGN in UV and X-rays simultaneously.

The most famous blazar observed is OJ 287, believed to contain a binary system of SMBH. This object was observed with AstroSat from 2017 to 2020 and was caught in three very different flux states tracing its source spectral evolution (see *Figure* 11). The 2017 observation showed activity driven by a new spectral component—a flat optical-UV spectrum and hard X-ray spectrum that disappeared in 2018 and re-emerged in 2020. The 2018 observation showed a flatter X-ray spectrum with a sharp decline or cutoff in the optical-UV band, which got revealed principally due to the simultaneous FUV data from AstroSat (see [23] and [26]).

Conclusions

AstroSat has studied all kinds of objects in the universe and made many discoveries since its launch in 2015. It has not been possible to list all the important results here. Until 2022, a total of ~140 papers based on UVIT, ~100 papers using the LAXPC, ~80 using the SXT, and ~30 (+ >400 Gamma-ray circulars) using the CZTI and associated instrumentation and performance have been published since the launch of AstroSat. Several papers published in the special issue titled *AstroSat: Five Years in Orbit* of the *Journal of Astrophysics and Astronomy*[3], also highlight many results and discoveries made by AstroSat.

[3] *JoAA*, Volume.42, Guest Eds: S. Seetha and D. Bhattacharya, 2021, https://www.ias.ac.in/listing/forthcoming/joaa

Acknowledgements

It is with great pleasure that I acknowledge the efforts of all the scientists and engineers at TIFR, IIA, IUCAA, ISRO, ISSDC, RRI, PRL, and several private contractors who made AstroSat a reality. The work of all the people at ISSDC and the Payload Operation Centres of individual payloads, who are scheduling obser-

vations round the clock, and providing data to all the observers, is cheerfully acknowledged. I also acknowledge all the users of AstroSat, and authors of the articles based on AstroSat observations, who have allowed me to reproduce some of their results and figures in this article.

Suggested Reading

[1] R Kumar, A C Pradhan, A Mohapatra, et al., Ultraviolet imaging telescope (UVIT) observation of the galactic globular cluster NGC 7492, *MNRAS*, 502, 313, pp.313–327, 2021.

[2] D S Prabhu, A Subramaniam, and S Sahu, The first extensive exploration of UV-bright stars in the globular cluster NGC 2808, *ApJ*, 908, 66, pp.1–19, 2021.

[3] S Pandey, A Subramaniam, and V V Jadhav, *MNRAS*, 507, 2373, 2021.

[4] S Lalitha, J H M M Schmitt, K P Singh, et al., Proxima Centauri-the nearest planet host observed simultaneously with AstroSat, Chandra and HST, *MNRAS*, 498, pp.3658–3663, 2020.

[5] K P Singh et al., Observations of bright stars with AstroSat soft X-ray telescope, *JoAA*, Vol.42, No.77, 2021.

[6] S Lalitha, U Pathak, K P Singh, 2022, (in preparation).

[7] K George, et al., Vol.A&A 614, A130, 2018.

[8] K George, et al., Vol.A&A 613, L9, 2018.

[9] K George, et al., *MNRAS*, 479, 4126, 2018.

[10] K Saha, S N Tandon, et al., *Nature Astronomy*, Vol.4, pp.1185–1194, 2022.

[11] S Bhattacharyya, K P Singh, G C Stewart et al., Science with the AstroSat soft X-ray telescope: An overview *JoAA*, Vol.42, No.17, 2021.

[12] M Pahari, S Bhattacharyya, A R Rao, et al., AstroSat and Chandra view of the high soft state of 4U 1630–47 (4U 1630–472): Evidence of the disk wind and a rapidly spinning black hole, *ApJ*, Vol.867, 86, 2018.

[13] S Bala, D Bhattacharya, R Staubert and C Maitra, Time evolution of cyclotron line of Her X-1: a detailed statistical analysis including new AstroSat data, *MNRAS*, Vol.497, No.1, pp.1029-–1042, 2020.

[14] S P Mudambi, A Rao, S B Gudennavar, R Misra and S G Bubbly, Estimation of the black hole spin in LMC X-1 using AstroSat, *MNRAS*, Vol.498, No.3, pp.4404–4410, 2020.

[15] J S Yadav, P C Agrawal, R Misra, et.al., LAXPC instrument onboard AstroSat: Five exciting years of new scientific results specially on X-ray binaries, *JoAA*, Vol.42, No.40, 2021.

[16] A Beri, S Naik, K P Singh et al., AstroSat observations of the first Galactic ULX pulsar Swift J0243.6+6124, *MNRAS*, Vol.500, No.1, pp.565–575, 2021.

[17] R Misra, D Rawat, J S Yadav, P Jain, Identification of QPO frequency of GRS 1915+105 as the relativistic dynamic frequency of a truncated accretion disk, *ApJ Letters*, Vol.889, L36 (6pp), 2020.

[18] K P Singh, V Girish, M Pavana et al., AstroSat soft X-ray observations of

the symbiotic recurrent nova V3890 Sgr during its 2019 outburst, *MNRAS*, Vol.501, No.1, pp.36–49, 2021.

[19] P Roy, A Beri and S Bhattacharyya, Thermonuclear X-ray bursts from 4U 1636-536 observed with AstroSat, *MNRAS*, Vol.508, No.2, pp.2123–2133, 2021.

[20] S V Vadawale, T Chattopadhyay, N P S Mithun et al., Phase-resolved X-ray polarimetry of the Crab pulsar with the AstroSat CZT Imager, *Nature Astronomy*, Vol.2, pp.50–55, 2018.

[21] A K Kembhavi and J V Narlikar, *Quasars and Active Galactic Nuclei: An Introduction*, Cambridge University Press, 1999.

[22] K P Singh, *BAAS*, 41, 137, 2013.

[23] P Kushwaha et al., AstroSat view of Blazar OJ 287: A complete evolutionary cycle of HBL Component from end-phase to disappearance and re-emergence, *Proceedings of Science*, 37th International Cosmic Ray Conference (ICRC 2021) July 12th–23rd, 2021, Online, Berlin, Germany, 2021.

[24] P Tripathi, G C Dewangan, I E Papadakis, and K P Singh, Revealing thermal comptonization of accretion disk photons in IC 4329A with AstroSat, *ApJ*, Vol.915, pp.25, 2021.

[25] S Chandra et al., X-Ray observations of 1ES 1959+650 in its high-activity state in 2016–2017 with AstroSat and Swift, *ApJ*, Vol.918, 67, 2021.

[26] K P Singh, P Kushwaha et al., Spectral states of OJ 287 blazar from multiwavelength observations with AstroSat, *MNRAS*, Vol.509, No.2, pp.2696-–2706, 2022.

Address for Correspondence
K P Singh
IISER Mohali
Knowledge City, Sector 81
SAS Nagar
Manauli PO 140 306, India.
Email:
kps@iisermohali.ac.in